THE JOURNAL OF BIOLOGICAL CHEMISTRY
Vol. 278, No. 47, Issue of November 21, pp. 46878–46885, 2003
Printed in U.S.A.

Binding of the C-terminal Sterile α Motif (SAM) Domain of Human p73 to Lipid Membranes*

Received for publication, July 21, 2003, and in revised form, September 3, 2003
Published, JBC Papers in Press, September 3, 2003, DOI 10.1074/jbc.M307846200

Francisco N. Barrera‡§, José A. Poveda‡, José M. González-Ros‡¶, and José L. Neira‡‖**

From the ‡Instituto de Biología Molecular y Celular, Universidad Miguel Hernández, 03202 Elche (Alicante), Spain and ‖Instituto de Biocomputación y Física de Sistemas Complejos, Universidad de Zaragoza, 50009 Zaragoza, Spain

The α splice variant of p73 (p73α), a homologue of the tumor suppressor p53, has close to its C terminus a sterile α motif (SAM), SAMp73, that is thought to be involved in protein-protein interactions. Here, we report the lipid binding properties of this domain. Binding was assayed against zwitterionic (phosphatidylcholine) and anionic (phosphatidic acid) lipids and was studied by different biophysical techniques, namely, circular dichroism and fluorescence spectroscopies and differential scanning calorimetry. These techniques unambiguously indicate that SAMp73 binds to lipids. The binding involves protein surface attachment and partial membrane penetration, accompanied by changes in SAMp73 structure.

p73 and p63 are members of the p53 gene family (1, 2). As the tumor suppressor p53, p73 and p63 are also transcription factors that contain an N-terminal transactivation domain, a sequence-specific DNA-binding domain, and an oligomerization domain with a high sequence homology to the corresponding domains of p53. For instance, p73 shares 63% identity with the DNA-binding region of p53 (including the conservation of all DNA-binding residues), 38% identity with the tetramerization domain, and 29% with the transactivation domain. Furthermore, p73 and p63 share a relative functional homology with p53, because they can both activate transcription from p53-responsive genes, stop the cell cycle, and induce apoptosis when overexpressed. Moreover, p73 is positively regulated in p53-deficient tumors in response to oncogene overexpression, and its expression is increased in several tumor types (1, 3–7). It seems that in the absence of p53, p73 can take its place and induce apoptosis in tumoral cells, although the ultimate role of p73 in tumor suppression is still unclear (5). Unlike p53, p73 and p63 are only rarely mutated in the large number of tumors examined to date and thus they are unlikely to be classical tumor suppressor genes. Also in contrast to p53, in mice lacking p73 there have been described severe developmental abnormalities, such as hippocampal dysgenesis, hydrocephalus, chronic infections, and inflammation, as well as abnormalities in pheromone sensory pathways; however, no increase in the tumor formation rate is detected (as it happened in p53 knockout mice (8)).

Conversely to p53, p73 and p63 contain additional C-terminal extensions. In both proteins, these extensions show alternative splicing, which results in at least six C-terminal variants for p73 (α–φ) and three for p63 (α–γ) (1, 9, 10). These isoforms have different transcription and biological properties, and their expression patterns change among normal tissues (9). For example, p73β transactivates many p53-responsive promoters, and p73α does so to a lesser extent (2–4). Nonetheless, the role of the several isoforms in cellular function is far from being fully understood, and it has been shown that their differential regulatory roles are highly cell context-dependent (11).

The α variants of p73 and p63 have close to their C terminus a SAM[1] domain, which is thought to be responsible for regulating p53-like functions (12). SAM domains are protein modules of ~65–70 amino acids found in diverse proteins whose functions range from signal transduction to transcriptional repression (12). Interestingly enough, it has been reported that the α isoform of p73 (and also that of p63) has its p53-like function dramatically reduced in comparison with other non-SAM-containing isoforms, suggesting that SAM domain could be responsible for those functional differences (12, 13). The structure of the SAM domain of p73, SAMp73 (the C-terminal region of the p73α protein comprising residues 487–554 of the intact protein), has been resolved by NMR (14) and x-ray crystallography (15, 16). The domain (residues 487–554 of the full p73α protein) contains a single tryptophan residue, which could be used as a spectroscopic probe to monitor the protein conformational changes. The structure of the domain reveals a small five-helix bundle composed of four α-helices (residues 491–499 (helix 1), 506–511 (helix 2), 525–531 (helix 4), and 538–550 (helix 5)) and a small 3_{10}-helix (residues 517–520 (helix 3)). The SAMp73 has structural similarity with two ephrin receptors tyrosine kinases (14), and the spatial arrangement of the bundle is similar to that of SAM domains found in other proteins (13). SAM domains are putatively considered to be responsible for regulating protein functions *via* self-association or by association with other domains (17), but the exact function of SAMp73 is not known. The crystal structure of SAMp73 reveals a dimeric organization (15), but the NMR

* This work was supported by Projects GV-00-024-5 (to J. L. N.) and CITIDIB/2002/6 (to J. L. N.) from Generalitat Valenciana, BIO2000-1081 (to J. L. N.) and BFI2002-03410 (to J. M. G.-R.) from the Spanish Ministerio de Ciencia y Tecnología, and Project FIS-01/0001–02 (JLN) from the Spanish Ministerio de Sanidad y Consumo. The costs of publication of this article were defrayed in part by the payment of page charges. This article must therefore be hereby marked "*advertisement*" in accordance with 18 U.S.C. Section 1734 solely to indicate this fact.

§ Recipient of a predoctoral fellowship from Generalitat Valenciana.

¶ To whom correspondence may be addressed: Instituto de Biología Molecular y Celular, Edificio Torregaitán, Universidad Miguel Hernández, Avda. del Ferrocarril s/n, 03202, Elche (Alicante), Spain. Tel.: 34-9666587571; Fax: 34-966658758; E-mail: gonzalez.ros@umh.es.

** To whom correspondence may be addressed: Instituto de Biología Molecular y Celular, Edificio Torregaitán, Universidad Miguel Hernández, Avda. del Ferrocarril s/n, 03202, Elche (Alicante), Spain. Tel.: 34-966658459; Fax: 34-966658758; E-mail: jlneira@umh.es.

[1] The abbreviations used are: SAM, sterile α motif; DMPA, 1,2-dimyristoyl-*sn*-glycero-3-phosphate; DMPC, 1,2-dimyristoyl-*sn*-glycero-3-phosphocoline; DSC, differential scanning calorimetry; PA, phosphatidic acid; PC, phosphatidylcholine; RET, resonance energy transfer; TMA-DPH, 1-(4-trimethylammoniumphenyl)-6-phenyl-1,3,5hexatriene.

structure is monomeric (14), suggesting that dimer formation in the crystal is an effect of crystal packing rather than a real physiological state; furthermore, equilibrium sedimentation experiments have shown that SAMp73 is monomeric under a wide range of experimental conditions (14, 18).

Because of its small size (67 residues long), we are using SAMp73 as a model for folding, stability, and macromolecular binding studies. We have embarked in the study of the interactions of SAMp73 with other macromolecules, namely proteins, nucleic acids, and lipids. Here, we explore its lipid binding properties toward PA (an anionic lipid) and PC (a zwitterionic lipid). The results indicate that SAMp73 interacts with both lipids. To the best of our knowledge, this study represents the first report of the lipid binding properties of a SAM domain, and it raises new questions about the role of this domain in p73 function.

EXPERIMENTAL PROCEDURES

Materials

Imidazole, Trizma base, and NaCl were from Sigma. The Ni^{2+}-nitrilotriacetic acid resin was from Invitrogen. Egg yolk PC and PA, DMPA, and DMPC were obtained from Avanti Polar lipids (Birminghman, AL). TMA-DPH was from Molecular Probes. Spectroscopy grade *N*,*N*-dimethylformamide was from Merck. Dialysis tubing was from Spectrapore, with a molecular mass cut-off of 3500 Da. Standard suppliers were used for all other chemicals. Water was deionized and purified on a Millipore system.

Protein Expression and Purification

The SAMp73 clone, comprising residues 487–554 of the intact p73α and a His_6 tag at the N terminus, was kindly donated by C. H. Arrowsmith. We have carried out all the studies with this construct because its structure is well known by NMR (14), and no differences were observed with that obtained by x-ray, where the His_6 tag had been removed (14–16). Recombinant protein was expressed in *Escherichia coli* C43 strain (19) and purified using Ni^{2+}-nitrilotriacetic acid chromatography. To eliminate any protein or DNA bound to the resin, co-eluting with the protein, an additional gel filtration chromatography step, was carried out by using a Superdex 75 16/60 gel filtration column (Amersham Biosciences) running on an AKTA FPLC system (Amersham Biosciences). Protein purity was larger than 95% as concluded from visual inspection in the SDS protein-denaturing gels and from matrix-assisted laser desorption ionization time-of-flight experiments (data not shown). The yield was 30–35 mg of protein/liter of culture. The samples were dialyzed extensively against 0.2 M NaCl, lyophilized, and stored at −80 °C. The protein concentration was calculated from the absorbance of a stock solution measured at 280 nm, using the extinction coefficients of model compounds (20).

Lipid Vesicles and Sample Preparation

Lipid vesicles were prepared by dissolving the required amount of lipid (PA, PC, DMPA, and DMPC) in chloroform/methanol (1:1 v/v) and drying, first under a gaseous nitrogen stream and then under vacuum for 3 h to remove all traces of organic solvents. The thin layer formed was resuspended in water (resulting in a 27 mM lipid concentration) while being vortexed and warmed gently (usually 10 °C over the T_c for DMPA and DMPC and at 55 °C for PA and PC). After lipid hydration, the PA and PC resulting multilamellar liposome suspensions were sonicated, using a Branson Sonifier model 250 fitted with a microtip (Branson, Shelton, CT) until a clear suspension of small unilamellar vesicles was obtained (typically 1 min for PA and 5 min, in bursts of 1 min, for PC while being cooled in ice). These preparations have been shown to yield vesicles with diameters ranging from 300 to 600 Å (21). The sonicated samples were then centrifuged in a microcentrifuge at 10,000 rpm for 2 min to remove any titanium particle shed from the microtip during sonication. No significant lipid pellet was observed after the centrifugation.

The lipid-protein samples were prepared by mixing the corresponding volumes of protein and lipid solutions, NaCl and Tris, pH 7; salt and buffer concentrations were carefully set to 200 and 10 mM, respectively, from 10-fold concentrated stocks, and the final volume was adjusted with water. All of the samples were mixed thoroughly and equilibrated usually for 20 min before the corresponding experiment was carried out. The pH of the samples was measured with an ultrathin Aldrich electrode in a Radiometer (Copenhagen) pH meter to discard differences between calculated and measured pH values.

Far-UV CD Measurements

Circular dichroism spectra were collected on a Jasco J810 spectropolarimeter fitted with a thermostated cell holder and interfaced with a Neslab RTE-111 water bath. The instrument was periodically calibrated with (+)10-camphorsulphonic acid. Isothermal wavelength spectra were acquired at a scan speed of 50 nm/min with a response time of 2 s and averaged over seven scans at 25 °C. Far-UV measurements were performed using 30 μM of protein in 10 mM of the above described buffer, using 0.1-cm-pathlength cells (Hellma). The corresponding backgrounds were subtracted from the final spectra, and they usually accounted less than the 5% of the sample ellipticities. Only at lipid concentrations over 5 mM were more intense backgrounds observed, but they never accounted for more than the 15% of the total protein ellipticity signal (data not shown). Subtracted spectra were smoothed avoiding alteration of spectral intensities. To further check that the measurements were not influenced by the scattering derived from the presence of the lipid, data were also analyzed without making subtractions, and similar results were obtained (data not shown). Ellipticities are expressed as mean residue ellipticities, [Θ], in units of deg cm^2 $dmol^{-1}$, according to Equation 1,

$$[\Theta] = \frac{\Theta}{10lcN} \quad \text{(Eq. 1)}$$

where Θ is the observed ellipticity, c is the molar concentration of the protein, l is the cell pathlength (in cm), and N is the number of amino acid residues in the sequence.

Fluorescence Measurements

Fluorescence spectra for SAMp73 were collected either on a SLM 8000 spectrofluorometer (Spectronics Instruments, Urbana, IL) interfaced with a Haake water bath or in a Cary Eclipse spectrofluorometer (Varian) interfaced with a Peltier cell. A 0.5-cm-pathlength quartz cell (Hellma) was used for measurements in the SLM spectrofluorometer, and a 1-cm-pathlength quartz cell (Hellma) was used in the Varian spectrofluorometer. All of the experiments were carried out at 25 °C.

Steady State Fluorescence Measurements—The protein samples were excited at 280 and 295 nm to characterize possible different behaviors of tryptophan and/or tyrosine residues (20). It was observed that both spectra were similar. The rest of the experiments were acquired by excitation at 280 nm. The slit width was 4 nm for the excitation light and 8 nm for the emission light; the integration time was 1 s, and the increment of wavelength was set to 1 nm between 310 and 400 nm. Blank corrections were made in all spectra. The protein concentration was 3 μM.

Resonance Energy Transfer (RET) Measurements—The efficiency of energy transfer (E) can be defined according to Equation 2 (22),

$$E = 1 - (IF/IF_o) \quad \text{(Eq. 2)}$$

where IF and IF_o are the fluorescence emission intensity of the donor in the presence and in the absence of the energy acceptor, respectively. Aliquots of a concentrated TMA-DPH stock (in *N*,*N*-dimethylformamide) were added to a cuvette containing the lipid-protein mixtures, and after 90 min of incubation, the changes of tryptophan emission fluorescence were monitored upon excitation at 280 nm. The effect of the acceptor (TMA-DPH) absorption at donor (tryptophan) emission maximum (340 nm) was corrected as described by Coutinho and Prieto (23). Monitoring of the emission wavelength at 330 nm (where TMA-DPH absorption is clearly reduced) yielded similar results (data not shown). No correction for the acceptor absorption at donor excitation wavelength was made because TMA-DPH absorbance at 280 nm was negligible. The extinction molar coefficient, ϵ, for TMA-DPH was that provided by Molecular Probes ($\epsilon = 75000\ M^{-1}\ cm^{-1}$). The slit width was 2 nm for the excitation light and 4 nm for the emission light.

The approach developed by Wolber and Hudson (24) was used to obtain the theoretical expected value for the efficiency of energy transfer in a bilayer two-dimensional system. This theoretical model represents an analytical solution of the Förster energy transfer problem when: (i) both the donors and acceptors are randomly distributed in a plane and (ii) donors are excluded from a region surrounding each

acceptor. According to this model, the relative quantum yield, q_r, is defined as follows.

$$q_r = 1 - E \quad \text{(Eq. 3)}$$

The relative quantum yield was theoretically calculated for different R_e/R_o ratios at increasing C values, where R_e is the distance between donor and acceptor at their closest approach, R_o is the critical radius of transfer (also defined as the distance at which the transfer efficiency is 50%), and C is the concentration of acceptors per R_o^2 (where the area of one PA molecule is 70 Å^2 and that of PC molecule is 80 Å^2). R_o was calculated according to the equations developed by Förster and others (25, 26),

$$R_o = 9876(J\kappa^2 n^{-4}\Phi_D)^{1/6} \quad (\text{in } Å) \quad \text{(Eq. 4)}$$

where J is the overlap integral, which measures the degree of overlap between the donor emission spectrum and the acceptor absorption spectrum; κ^2 is the orientation factor, which was taken to be 2/3 (27); n is the refractive index of the medium, which was taken as 1.44 (that is, the value of the bilayer interior) (28); and Φ_D is the quantum yield of the donor in the absence of acceptor. The quantum yield of the sole tryptophan was determined using 5-metoxiindole as a quantum yield standard, as described by Lakowicz (29). In the presence of PA, the calculated Φ_D was 0.228, and in the presence of PC, Φ_D was 0.179. The overlap integral, J, was calculated by Equation 5,

$$J = \frac{\int f_D(\lambda)\varepsilon_A(\lambda)\lambda^4 d\lambda}{\int f_D(\lambda)\, d\lambda} \quad (\text{in } M^{-1}\,cm^3) \quad \text{(Eq. 5)}$$

where $f_D(\lambda)$ is the donor fluorescence intensity at each wavelength, λ, and $\epsilon_A(\lambda)$ is the acceptor molar extinction coefficient at each wavelength. The absorption spectra were taken in a Beckman DU 640 spectrophotometer.

Partition Coefficient Determination

A parameter that can be used to quantify the extent of lipid-protein interactions is the partition coefficient, K_p, which is described by the following equation,

$$K_p = \frac{n_l/V_l}{n_w/V_w} \quad \text{(Eq. 6)}$$

where n_l is the number of moles of the protein in lipid, n_w is the number of moles of the protein in aqueous solution, V_l is the volume of the lipid phase, and V_w is the volume of aqueous phase. The variation in a spectroscopic parameter, if it is proportional to the concentration of protein bound to the membrane, can be used to determine the lipid partition coefficient according to Refs. 30 and 31,

$$X = \frac{X_{max}K_p\gamma[\text{lipid}]}{1 + K_p\gamma[\text{lipid}]} \quad \text{(Eq. 7)}$$

where X is the spectroscopic parameter that changes upon addition of increasing amounts of lipid (in our studies, the [Θ], or the fluorescence emission maximum and the fluorescence intensity); X_{max} is the maximum value of X, and γ is the molar volume of the lipid (which has values of 0.7 M^{-1} for PA and 0.8 M^{-1} for PC (32)). Fitting by nonlinear least squares analysis was carried out by using the general curve fit option of Kaleidagraph (Abelbeck software) on a personal computer.

Differential Scanning Calorimetry

DSC experiments were performed with a MicroCal MC-2 (Microcal Inc., Northampton, MA) differential scanning calorimeter interfaced to a computer equipped with a Data Translation DT-2801 A/D converter board for instrument control and automatic data collection. The samples were prepared as described (see before), but DMPA-containing samples were prepared with 0.1 mM EDTA to avoid perturbations in the phase transition created by the presence of Ca^{2+}. NaCl concentration was carefully kept constant to avoid artifacts caused by the positive ions during the DMPA phase transition. The samples were degassed under vacuum for 10 min with gentle stirring prior to being loaded into the calorimetric cell. Differences in the heat capacity between the sample and the reference cell, filled with buffer solution, were obtained by raising the temperature at a constant rate of 60 °C/h over a temperature range of 10–60 °C. At these temperatures thermal unfolding of the protein is not expected (18). The excess heat capacity functions were obtained after base-line subtraction and correction for the instrument time response. A series of three consecutive scans were at least acquired to ensure scan-to-scan reproducibility. Although the second and third scans were identical, only the third scan was used for calculation of the transition temperature and the enthalpy. The Microcal Origin software was used for data acquisition and analysis.

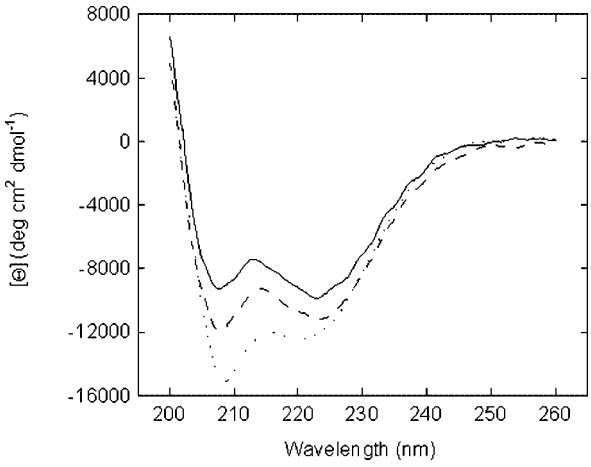

FIG. 1. **Far-UV CD spectra of SAMp73 in lipids.** The far-UV CD spectra at different solvent conditions are indicated: SAMp73 in solution (*continuous line*), SAMp73 in PC (*dashed line*), and SAMp73 in PA (*dotted line*). The lipid concentration was 3 mM. The protein concentration was 30 μM. The spectra were acquired in 0.1-cm-pathlength cells. The conditions were 10 mM Tris, pH 7, 0.2 M NaCl, 25 °C. The spectra were not corrected by the molar fraction of the SAMp73 inserted into the membrane and that remaining in the aqueous phase.

RESULTS

Far-UV CD Experiments

We used far-UV CD in the analysis of the protein-lipid binding as a spectroscopic probe that is sensitive to protein secondary structure (33, 34). SAMp73 in solution shows an intense far-UV CD spectrum with the features of an α-helical protein, with minima at 222 and 208 nm (Fig. 1), although interference from the aromatic residues cannot be ruled out (33, 34). To study the lipid binding properties of SAMp73, we first tested whether its CD spectrum changed upon incubation with either anionic (PA) or zwitterionic (PC) lipid membranes. It was observed that the negatively charged lipid vesicles of PA induced a significant change in the SAMp73 CD spectrum, with a marked increase in the ellipticity (in absolute value) at 222 nm and a larger change in that at 208 nm (Fig. 1). The latter could indicate either an increase in the random coil population or changes in the environment of the aromatic residues (33, 34). Binding of the protein to zwitterionic PC vesicles induced also an enhancement in the ellipticity of the SAMp73 spectrum, but its extent was smaller than that observed in PA. In this case, the ellipticity at 208 and 222 nm increased to nearly the same extent.

The partition coefficients, K_p, obtained from the ellipticity changes at 208 nm upon increase in lipid concentration were 1360 ± 190 for PA and 3967 ± 970 for PC (Fig. 2) (Equation 6). Similar partition coefficients were also determined from the ellipticity changes at 222 nm. These partition coefficients allowed us to determine the population of SAMp73 distributed between the aqueous and lipid phases at a given lipid concentration. The molar fraction of a protein in the aqueous solution, X_w, can be calculated as follows (35).

$$X_w = \frac{1}{1 + K_p\gamma[\text{lipid}]} \quad \text{(Eq. 8)}$$

For instance, in PC at 3 mM, the percentage of SAMp73 in the aqueous phase was 9.5%, whereas for PA at 3 mM, it was 26%.

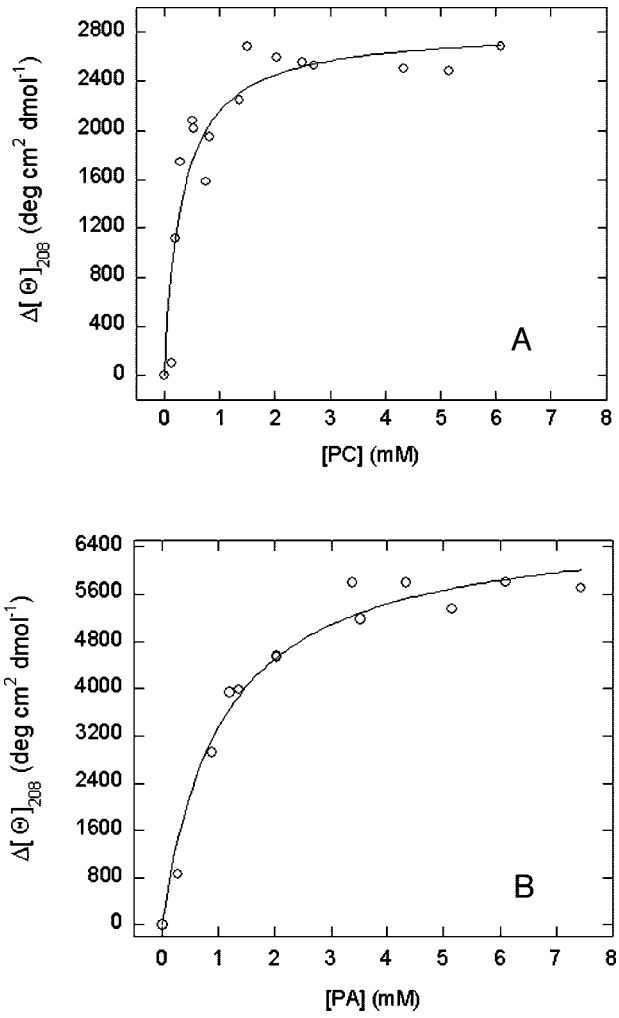

FIG. 2. **Binding constant determination by CD.** Mean residue ellipticity changes at 208 nm ($\Delta[\Theta]_{208}$) were followed at increasing lipid concentration in PC (*A*) and PA (*B*). K_p values were obtained by fitting to Equation 6 (*solid lines*). The protein concentration was 30 μM. The conditions were 10 mM Tris, pH 7, 0.2 M NaCl, 25 °C.

Fluorescence Experiments

Steady State Measurements—The intrinsic protein fluorescence is a highly sensitive probe to monitor protein-lipid binding (36–38). SAMp73 has one tryptophan and five tyrosine residues. Trp^{542}, in the numbering of intact p73α, is in the middle of helix 5 forming the hydrophobic core of the protein; Tyr^{487} is the N-terminal residue; Tyr^{508} is in the middle of helix 2; Tyr^{518} and Tyr^{537} are at the beginnings of helices 3 and 5, respectively; and Tyr^{554} is the C-terminal residue. The emission fluorescence spectrum of native SAMp73 is dominated by the emission of the sole tryptophan residue (18), with a maximum at 336 nm at neutral pH, which indicates that the tryptophan is partially buried within the protein structure, as concluded from the x-ray (15, 16) and NMR structures (14).

In the presence of either PC or PA, emission maxima were shifted toward 339 or 340 nm, respectively, in a highly reproducible manner (Fig. 3). The fluorescence intensity also increased, being this change larger in the presence of PA. The changes observed in both parameters, as the lipid concentration increased, were also used to obtain the partition coefficients (Equation 6). The K_p values obtained were similar to those determined above from the CD data (data not shown).

Resonance Energy Transfer Measurements—The TMA-DPH probe has been used as an acceptor in energy transfer studies because its absorbance spectrum overlaps with the protein

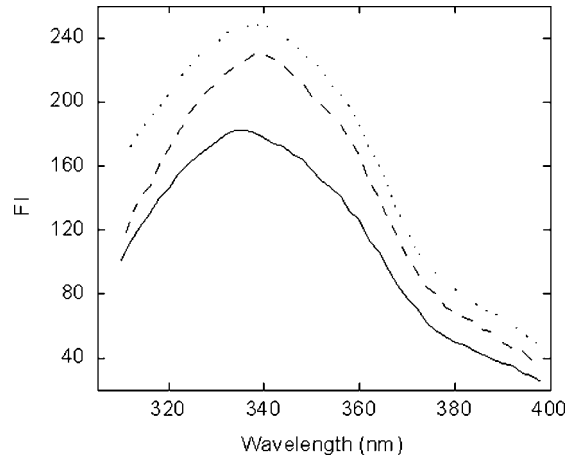

FIG. 3. **Fluorescence changes of SAMp73 upon lipid binding.** Representative emission spectra (λ_{ex} = 280 nm) of SAMp73 in solution (*continuous line*), SAMp73 in PC (*dashed line*), and SAMp73 in PA (*dotted line*). The lipid and protein concentrations were 3 mM and 3 μM, respectively. Fluorescence intensity (*FI*) was in arbitrary units. The spectra were acquired in 0.5-cm-pathlength cells. The conditions were 10 mM Tris, pH 7, 0.2 M NaCl, 25 °C. The spectra were not corrected by the molar fraction of the SAMp73 inserted into the membrane and that remaining in the aqueous phase.

emission spectra (22, 38). This amphipatic probe has a positively charged group attached to one of its two phenyl terminal groups, and it partitions almost exclusively into the membrane. When embedded in lipid membranes, the positive charged group is anchored to the lipid polar interfacial region, whereas the rest of the molecule is located into the hydrophobic interior of the membrane, with an averaged position parallel to the phospholipid acyl chains (38).

The fluorescence emission of samples containing SAMp73 and lipid was significantly quenched by the presence of TMA-DPH in a concentration-dependent manner. Furthermore, the characteristic emission spectrum of TMA-DPH (with a maximum at 430 nm) was progressively observed, under our conditions, as a consequence of the energy transfer (Fig. 4*A*). These results suggest that some interaction between SAMp73 and the membrane (where TMA-DPH is located) must exist, because the energy transfer process is not significant at distances larger than 100 Å (29).

To determine the extent of the insertion of SAMp73 into the lipid bilayer from the RET data, we used the theoretical approach of Wolber and Hudson (24), where distances between donor and acceptor can be obtained as a function of R_o. The calculated R_o values for the resonance energy transfer between Trp^{542} and TMA-DPH were 34.1 Å in PC and 36.9 Å in PA (see "Experimental Procedures"). These values are similar to the typical R_o values for the tryptophan-TMA-DPH pair (29). From the decrease in the fluorescence intensity, the efficiency of energy transfer, E, and the relative quantum yield, q_r, were determined, and the latter was plotted against the density of acceptors expressed in terms of C (that is, the number of TMA-DPH molecules in an area of membrane equivalent to R_o^2) (Fig. 4*B*). The experimental values were compared with those theoretically obtained for different R_e/R_o ratios, being closer to the theoretical lines corresponding to R_e/R_o values of 0 and 0.25 in the presence of either PA or PC (Fig. 4*B*). These findings indicate that R_e, the distance of the closest approach between donor and acceptor, is, within experimental error, in the range of 0–9.2 Å. TMA-DPH is located at 10.9 Å from the center of the bilayer (39) and then at a distance approximately 4–5 Å from the membrane interface. We can conclude from these data that SAMp73 is located in the membrane. Because the results obtained for both lipid vesicles (either negatively charged or zwit-

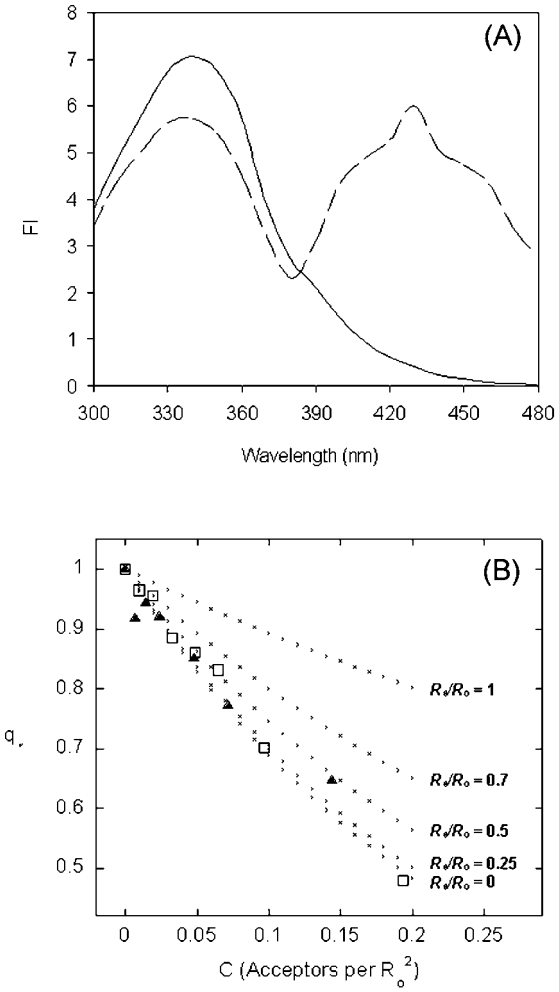

FIG. 4. **Resonance energy transfer measurements.** *A*, representative fluorescence spectra of SAMp73 in PA in the absence (*continuous line*) and in the presence of TMA-DPH (*dashed line*) (similar spectra were obtained with PC; data not shown). The molar ratio between the TMA-DPH and the lipid was 1:1200. The presence of the probe is shown by the signals appearing at 430 nm. Fluorescence intensity (*FI*) was in arbitrary units. The data were neither corrected by the molar fraction of the SAMp73 inserted into the membrane and that remaining in the aqueous phase nor by the TMA-DPH absorption at the tryptophan emission. *B*, RET between the SAMp73 tryptophan (donor) and TMA-DPH (acceptor), when the protein was in presence of PC (*filled triangles*) and PA (*open squares*) lipid membranes. The crosses represented the q_r values theoretically obtained for different R_e/R_o ratios. The lipid and protein concentrations were 3 mM and 3 μM, respectively. The conditions were 10 mM Tris, pH 7, 0.2 M NaCl, 25 °C. The data were corrected by the molar fraction of the SAMp73 inserted into the membrane and that remaining in the aqueous phase.

terionic) were analogous, the depth of the insertion of the protein into the two different membranes must also be similar.

DSC Experiments

DSC was also used to monitor the binding of SAMp73 to anionic and zwitterionic membranes, because it is known that the type of interaction with the lipid and the degree of penetration of a protein into the lipid bilayer affects the thermotropic behavior of the lipid phase transition (40–42). The dimyristoylated forms of PA and PC, DMPA and DMPC, respectively, which exhibit a cooperative phase transition at mild temperatures, were selected for these experiments. In the absence of protein, DSC scans of both lipids showed a sharp peak corresponding to the their main phase transition, accompanied in the case of DMPC by a minor peak at lower temperatures, the so-called pretransition (Fig. 5). The apparent enthalpies (ΔH), estimated from the area under the peak, and T_c, the temperature at the peak maximum of the main phase transition, were similar to those found by other authors (40, 41). The presence of SAMp73 influenced the thermotropic properties of both lipids. A loss of cooperativity and a reduction of the maximum heat capacity (C_p) for the main lipid phase transition of DMPC was observed. A slight shift to upper temperatures of the pretransition was also detected. In the presence of SAMp73, the main phase transition of DMPA occurred at a slightly lower T_c, and the maximum value of C_p was reduced. The peak became wider, and a loss of cooperativity was observed during the process. Remarkably, the enthalpy of the main lipid phase transition is not significantly changed in either lipid upon addition of the protein (Fig. 5).

DISCUSSION

Binding of SAMp73 to Lipid Membranes—SAM domains were first described as a module present in a small group of yeast sexual differentiation and *Drosophila* polyhomeotic proteins (43). These domains were subsequently found in other proteins involved in the regulation of numerous developmental processes among eukaryotes, suggesting that SAM domains were evolutionarily conserved. These domains tend to oligomerize, forming either homooligomers or heterooligomers, sometimes with non-1:1 stoichiometries, and their interactions with proteins lacking SAM domains have also been described (44). Moreover, some SAM domains are known to self-associate using multiple binding protein surfaces to generate polymeric structures (45).

Recently, however, the SAM domain of p73, SAMp73, has been shown to be monomeric in solution (14, 18). Furthermore, although the SAM domains of EphA4 and B2 receptors formed oligomers, oligomerization was not observed for both receptors (17, 46). Thus, the function of the SAM domains does not seem to be restricted to oligomer formation, and it can be variable.

Here, we have shown by using CD, fluorescence, and DSC measurements that SAMp73 clearly interacts with model membranes. Our CD results show that SAMp73 changes its structure upon binding to lipid membranes. This binding seems to alter the structure of the protein, and these changes are more important in PA than in PC membranes, suggesting possible differences in the structure of SAMp73 when bound to anionic or zwitterionic membranes. SAMp73 binds to PA and PC membranes with K_p values of 1360 ± 190 and 3967 ± 970, respectively; these values are similar to those reported in other lipid-protein bindings (35, 47). Similar partition coefficients were obtained by using fluorescence, but in this case the measurements showed larger associated errors, possibly because of the smaller extent of the fluorescence changes observed.

RET measurements between the membrane probe TMA-DPH and SAMp73 also demonstrate the protein-lipid interaction. These experiments show that R_e, the distance of closest approach between the sole tryptophan of SAMp73 and TMA-DPH, either in PC or PA membranes, is in the range 0–9.2 Å. Because TMA-DPH is located at 4–5 Å inside the membrane and because the thickness of an average bilayer is ~60 Å (~30 Å for hydrocarbon core and ~15 Å for each interfacial region) (39), these data are compatible with a peripheral location of the sole tryptophan of SAMp73 in the membrane.

The appreciable effect of SAMp73 on the thermotropic behavior of both DMPC and DMPA and its dependence with the amount of protein added further support the idea of an interaction between this protein and zwitterionic and anionic lipid membranes. Qualitatively, the major effects detected on the main lipid phase transition upon addition of the protein were quite similar in both lipids: (i) loss of cooperativity and (ii) diminution of the maximum heat capacity (C_p). Moreover, for

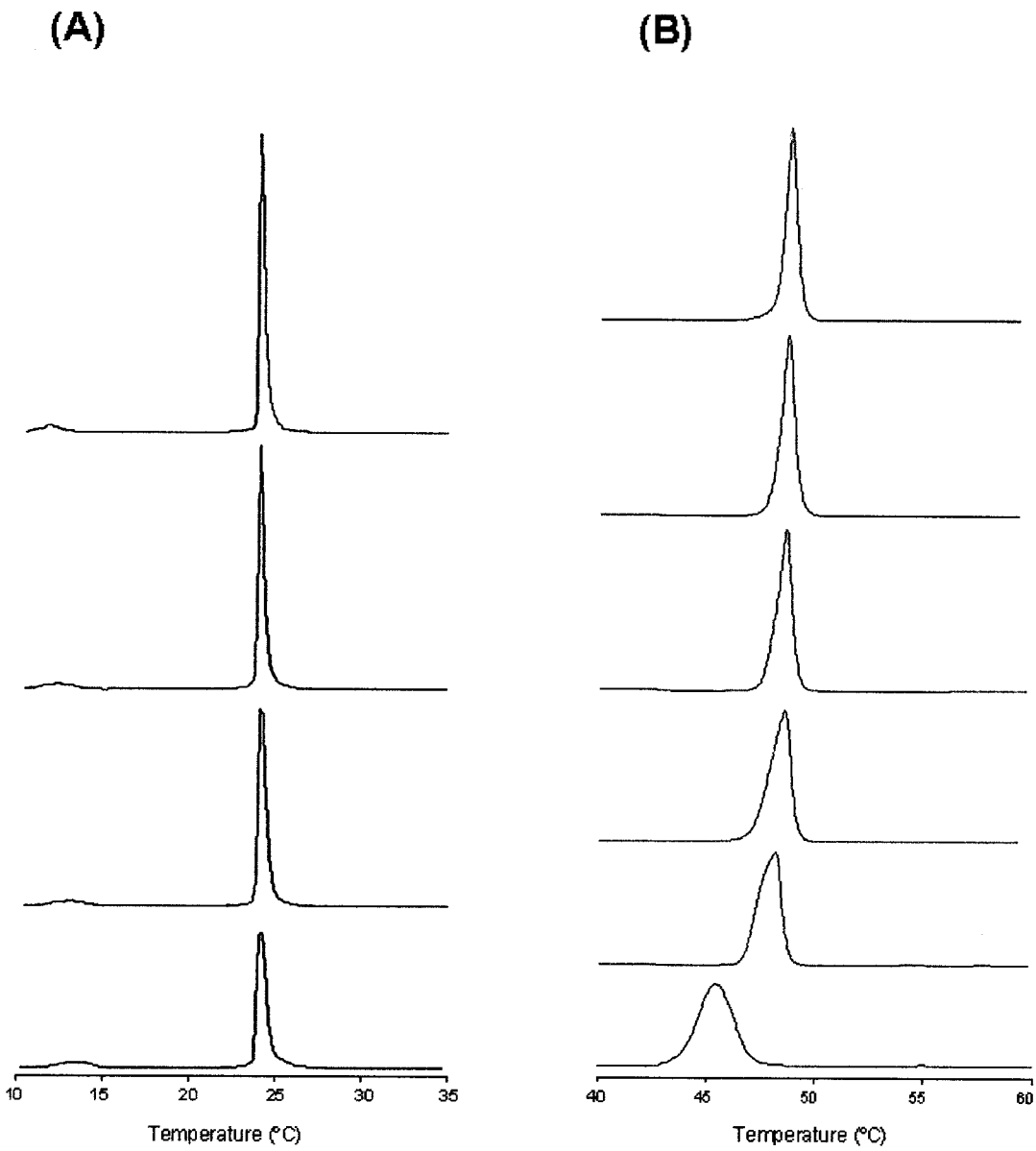

FIG. 5. **Differential scanning calorimetry of DMPA and DMPC.** *A*, DMPC; *B*, DMPA. From *top* to *bottom*, increasing amounts of protein were added to a fixed lipid concentration yielding the following lipid to protein molar ratios: no protein, 35:1, 22:1, and 13:1 in DMPC and no protein, 115:1, 64:1, 37:1, 27:1, and 17:1 in DMPA. The conditions were 10 mM Tris, pH 7, 0.2 M NaCl (and 0.1 mM EDTA for DMPA experiments).

DMPA, the lipid phase transition broadens, and the T_c value is reduced from 49 to 46 °C (Fig. 5). However, the enthalpy of the lipid phase transition is not significantly changed in any case, even at molar lipid to protein ratios of approximately 15:1 (although the exact lipid to bound-protein molar ratio is not known for these membranes under these temperatures). This probably means that there is not a large degree of penetration of SAMp73 in either DMPA or DMPC vesicles. In this view, it is likely that few phospholipid molecules are affected by the protein, and probably those affected can still participate in the phase transition; then small changes should be expected when compared with the DSC measurements carried out in the absence of protein, as observed.

Structural Changes of Membrane-bound SAMp73—Binding of SAMp73 to lipid membranes results in significant structural changes. The far-UV CD indicates that the helical content of SAM p73 increases in the presence of both lipids (although alterations in the CD spectrum caused by changes in the environment of the aromatic residues cannot be ruled out). These changes were larger for the anionic lipid (Fig. 1), and they were even larger when data were corrected by the molar fraction of protein present in the lipid phase (Equation 7) (data not shown). The increase in helical content is accompanied by an increase in the fluorescence intensity and solvent exposure of the tryptophan moiety, as concluded from the red shift in the fluorescence emission spectra (Fig. 3). Usually, upon lipid binding, the fluorescence spectra of proteins experience a blue shift caused by the highly hydrophobic lipid environment (21). Because Trp^{542} is partly buried, lipid binding must promote conformational changes involving the indole moiety and causing a more pronounced solvent exposure (responsible of the red shift change).

Because SAMp73 is a highly compact protein, which buries a large amount of hydrophobic surface (14, 18), how can SAMp73 bind lipids? Which are the protein-interacting regions? To try to answer these questions, we have used the method developed by White and Wimbley (48) to calculate putative protein-membrane interacting regions. Using windows of either 7, 9, or 11 amino acids, this approach has showed that two segments of the protein, those comprising residues 492–499 and residues

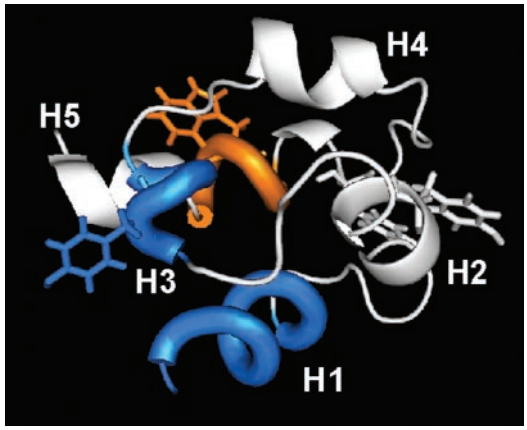

FIG. 6. **Location of the putative membrane-interacting regions in the SAMp73 NMR solution structure.** Regions with predicted membrane location (48) are represented as *cylinders*. The zone with interfacial tendency is *orange*, and those with tendency to be either in the interfacial region or in the interior of the membrane are *blue*. Tryptophan and tyrosine residues are depicted as *sticks*. The two N- and C-terminal residues are not shown (including Tyr^{487} and Tyr^{554}), because they are highly mobile zones whose precise situation is not defined in the NMR structure (14). The figure was obtained with PyMOL (60). The numbering of the helices according to location is indicated. *H1*, residues 491–499; *H2*, 506–511; *H3*, 517–520 (the 3_{10} helix); *H4*, 525–531; *H5*, 538–550.

517–521, were thermodynamically favored to be located both in the hydrophobic hydrocarbon core and in the membrane interfacial region. A third zone, comprising residues 540–544, was favored to be located in the interfacial region (Fig. 6). The first region comprises basically helix 1, which is highly hydrophobic, ^{492}SLVSFLTG^{499}; the second zone involves the 3_{10} helix and a interhelical residue between this helix and the helix 4, with the sequence ^{517}IYHLQ^{521}; and finally, the third region comprises a portion of the helix 5, with the sequence ^{540}TIWRG^{544}, including the sole tryptophan of the protein. It is interesting to note that although the different predicted regions are very short, they are in close proximity to each other in the three-dimensional structure of SAM.

The locations of those three regions in the SAMp73 structure (Fig. 6) suggest that at least small structural rearrangements upon lipid binding are necessary to fully accomplish with their predicted membrane location. The experimental structural changes indicated by the CD and fluorescence could be reporting this process, indicating a slightly different rearrangement when the protein binds to either PA or PC membranes. If upon lipid binding the tertiary organization of the domain was not substantially altered, the aromatic residues of the domain would locate in the interfacial region of the membrane, influencing the precise interfacial positioning of SAMp73, as it happens in other proteins (49–52). However, we cannot rule out, based in our experimental results, the possibility that the entire protein as a whole is responsible for lipid binding. In this scenario, larger conformational rearrangements would probably occur.

To further determine the implications of our findings in the SAM family function, we decided to study the theoretical membrane binding propensities of 29 different SAM domains found in a wide variety of proteins and species. For this purpose, we also used the method developed by White and co-workers (48, 50) and three different transmembrane segment prediction methods, those provided by Antheprot (51), TMpred (52), and dense alignment surface method (53). Of the 29 SAM domains, only in three of them, those from p73α and p63α, and the SAM domain of Cask-interacting protein 1 (54), were putative membrane-interacting regions predicted. In the case of SAMp73, the three transmembrane methods predicted an unique transmembrane region (comprising helix 1), and a transmembrane tendency was observed for the region corresponding to the 3_{10} helix but with nonsignificant scores. In the SAM domain of p63α, the method of White and co-workers predicted the same membrane propensities for the homologous regions of SAMp73; Antheprot and DAS gave positive results for the region homologous to the SAMp73 helix 1, and TMpred predicted with nonsignificant scores a transmembrane propensity for this region. Again, the three transmembrane prediction methods detected a nonrepresentative transmembrane tendency for the region homologous to the 3_{10} helix of SAMp73. In the case of Cask-interacting protein 1, only the method of White and co-workers predicted a significant transmembrane propensity in a region homologous to the first helix of SAMp73. To sum up, the theoretical results suggest that SAMp73 (and its homologue SAMp63) have a strong tendency to interact with membranes.

It seems that a functional divergence among SAM domains of p73α and p63α and those other SAM domains with reported protein-binding function could exist, although it cannot be ruled out that the SAM domains of p73α and p63α could be able to interact with other proteins also. Interestingly enough, these results suggest a parallelism between SAM domains and protein kinase C conserved 1 (C1) and protein kinase C conserved 2 (C2) domains. C1 and C2 domains are found in a wide range of proteins and have diverged evolutionarily into a family of versatile protein modules with diverse functions (55). These domains are able to bind to multiple proteins involved in protein regulation, but they can also bind to either anionic or zwitterionic membranes in a peripheral way (55).

Artifact or Real Lipid-Protein Binding?—After discussion of our findings, a question can be raised: Are the results described here biologically relevant? It is generally accepted that the SAM domains are involved in formation of homooligomers or heterooligomers. Furthermore, to date, the best described function of SAM domains is the head-to-tail polymer formation (45, 56, 57). However, recently, it has been shown that the SAM domain of Smaug interacts with RNA by resolving the x-ray structure of the complex (58). The interaction is not an artifact of the crystallization process because genetic analysis (58) and homology modeling and site-directed mutagenesis (59) also supported the structural results. Furthermore, it has also been shown that the SAM domain of the Vts1 protein of *Saccharomyces cerevisiae* also binds RNA with the same specificity as that of the Smaug protein (59). Both studies agree in their general conclusions; in both SAM domains, there is a spatially close patch of electropositive residues (involved in different elements of the secondary structure of both proteins) that define the RNA-binding site (58, 59). Interestingly enough, the RNA-binding region of the Smaug SAM domain involves a few amino acid residues of the α-helix 1 and the N terminus of α-helix 5 of both domains. In SAMp73, there is, conversely, a spatially close patch of highly hydrophobic regions (involving similar elements of secondary structure) that seems to define the lipid-binding site. Here, we have not been able to characterize at atomic detail (either NMR or x-ray) the structure of the SAMp73 in the presence of lipids, nor, to the best of our knowledge, have we been able to find reports either *in vivo* or *in vitro* on possible interactions among SAM domain and lipids. However, there are three independent lines of evidence suggesting that the results shown here are not a mere artifact: (i) the fact that several prediction algorithms (as happens with the genetic analysis in the case of the Smaug SAM domain) agree among them with the similar transmembrane predicted regions; (ii) different techniques that map different biophysical properties (secondary structure (CD), tertiary structure (fluo-

rescence), heat capacity of binding (DSC), and the energy transfer between the tryptophan of the protein and a membrane-embedded probe (RET)) unambiguously show the lipid-protein interaction; and (iii) similar binding results are found with lipids of different properties (PA and PC). It seems, as has been indicated (60), that the as yet characteristic protein interaction domains can also be used in other cell functions. Based on all these results, it is tempting to suggest that in SAM domains, the domain can be used as a general scaffold, which can function with several roles.

To conclude, the exact functions of the p73 protein are still a matter of discussion, but because: (i) it has been reported that p73α (and also p63α) has its p53-like function dramatically reduced in comparison with other non-SAM-containing isoforms and (ii) it seems (from our theoretical analysis here) that there is a functional divergence among SAMp73 and other SAM domains, our results suggest that the membrane-association properties of SAMp73 might be responsible for those functional differences (12, 13).

Acknowledgments—We deeply thank Prof. C. H. Arrowsmith for the kind gift of the SAMp73 clone and Drs. A. Pineda-Lucena, A. Ferrer-Montiel, F. J. Gómez, and C. R. Mateo for helpful suggestions and advice. We gratefully acknowledge May García, María Carmen Fuster, and Javier Casanova for excellent technical assistance.

REFERENCES

1. Kaghad, M., Bonnet, H., Yang, A., Creancier, L., Biscan, J. C., Valent, A., Minty, A., Chalon, P., Lelias, J. M., Dumont X., Ferrara, P., McKeon, F., and Caput, D. (1997) *Cell* **90,** 809–819
2. Jost, C. A., Marin, M. C., and Kaelin, W. G., Jr. (1997) *Nature* **389,** 191–194
3. Zhu, J., Jiang, J., Zhou, W., and Chen, X. (1998) *Cancer Res.* **58,** 5061–5065
4. Di Como, C. J., Gaiddon, C., and Prives, C. (1999) *Mol. Cell Biol.* **19,** 1438–1449
5. Zaika, A., Irwin, M., Sansome, C., and Moll, U. M. (2001) *J. Biol. Chem.* **276,** 11310–11316
6. Yang A., Kaghad M., Wang Y., Gillett E., Fleming M. D., Dotsch V., Andrews N. C., Caput D., and McKeon F. (1998) *Mol. Cell* **2,** 305–316
7. Strano, S., Munarriz, E., Rossi, M., Cristofanelli, B., Shaul, Y., Castagnoli, L., Levine, A. J., Sacchi, A., Cesareni, G., Oren, M., and Blandino, G. (2000) *J. Biol. Chem.* **275,** 29503–29512
8. Yang, A., Walker, N., Bronson, R., Kaghad, M., Oosterwegel, M., Bonnin, J., Vagner. C., Bonnet, H., Dikkes, P., Sharpe, A., McKeon, F., and Caput, D. (2000) *Nature* **404,** 99–103
9. De Laurenzi, V., Costanzo, A., Barcaroli, D., Terrinoni, A., Falco, M., Annicchiarico-Petruzzelli, M., Levero, M., and Mellino, G. (1998) *Exp. Med.* **188,** 1763–1768
10. Irwin M. S., and Kaelin W. G. (2001) *Cell Growth Differ.* **12,** 337–349
11. Freebern, W. J., Smith, J. L., Chaudhry, S. S., Haggerty, C. M., and Gardner, K. (2003) *J. Biol. Chem.* **278,** 2249–2255
12. Bork, P., and Koonin, E. V. (1998) *Nat. Genet.* **18,** 313–318
13. Thanos, C. D., and Bowie, J. U. (1999) *Protein Sci.* **8,** 1708–1710
14. Chi, S.-W., Ayed, A., and Arrowsmith, C. H. (1999) *EMBO J.* **18,** 4438–4445
15. Wang, W. K., Proctor, M. R., Buckle, A. M., Bycroft, M., and Chen, Y. W. (2000) *Acta Crystallogr. Sect. D Biol. Crystallogr.* **56,** 769–771
16. Wang, W. K., Bycroft, M., Foster, N. W., Buckle, A. M., Fersht, A. R., and Chen Y. W. (2001) *Acta Crystallogr. Sect. D Biol. Crystallogr.* **57,** 545–551
17. Schultz, J., Pointing, C. P., Hoffmann, K., and Bork, P. (1997) *Protein Sci.* **6,** 249–253
18. Barrera, F. N., Garzon, M. T., Gomez, F. J., and Neira, J. L. (2002) *Biochemistry* **41,** 743–753
19. Miroux, B., and Walker, J. E. (1996) *J. Mol. Biol.* **260,** 289–298
20. Pace, C. N., and Scholtz, J. M. (1997) in *Protein Structure* (Creighton, T. E., ed) 2nd Ed., pp. 253–259, Oxford University Press, Oxford
21. Sanghera, N., and Pinheiro, T. J. T. (2002) *J. Mol. Biol.* **315,** 1241–1256
22. Ferrer-Montiel, A., González-Ros, J. M., and Ferragut, J. A. (1988) *Biochim. Biophys. Acta* **937,** 379–386
23. Coutinho, A., and Prieto, M. (1993) *J. Chem. Ed.* **70,** 425
24. Wolber, P. K., and Hudson, B. S. (1979) *Biophys. J.* **28,** 197–210
25. Förster, T. (1959) *A. Naurforsch. A. Astrophys. Phys. Chem.* **4,** 321–327
26. Rapaport, D., and Shai, Y. (1992) *J. Biol. Chem.* **267,** 6502–6509
27. Stryer, L. (1978) *Annu. Rev. Biochem.* **47,** 819–846
28. Davenport, J., Dale, R. E., Bisby, R. H., and Cundal, R. B. (1985) *Biochemistry* **24,** 4097–4108
29. Lakowicz, J. R. (1999) *Principles of Fluorescence Spectroscopy*, 2nd Ed., Kluwer Academic/Plenum Press, New York
30. Eftink, M. R. (1997) *Methods Enzymol.* **278,** 221–257
31. Mateo, C. R., Prieto, M., Micol, V., Shapiro, S., and Villalaín, J. (2000) *Biochim. Biophys. Acta* **1509,** 167–175
32. Marsh, D. (1990) *CRC Handbook of Lipid Bilayers*, CRC Press, Boca Raton, FL
33. Woody, R. W. (1995) *Methods Enzymol.* **246,** 34–71
34. Kelly, S. M., and Price, N. C. (2000) *Curr. Protein Peptide Sci.* **1,** 349–384
35. Contreras, L. M., de Almeida, R. F., Villalaín, J., Fedorov, A., and Prieto, M. (2001) *Biophys. J.* **80,** 2273–2283
36. Surewicz, W. K., and Epand, R. M. (1984) *Biochemistry* **23,** 6072–6077
37. Rankin, S. E., Watts, A., and Pinheiro, T. J. T. (1998) *Biochemistry* **37,** 12588–12595
38. Prendergast, F. G., Haugland, R. P., Callahan, P. J., and Bodeau, D. (1981) *Biochemistry* **20,** 7333–7400
39. Kaiser, R. D., and London, E. (1998) *Biochemistry* **37,** 8180–8190
40. Papahadjopoulos, D., Moscarello, M., Eylara, E. H., and Isac, T. (1975) *Biochim. Biophys. Acta* **401,** 317–335
41. Ghosh, A. K., Rukmini, R., and Chattopadhyay, A. (1997) *Biochemistry* **36,** 14291–14305
42. Garidel, P., Johann, C., and Blume, A. (1997) *Biophys. J.* **72,** 2196–2210
43. Ponting, C. P. (1995) *Protein Sci.* **4,** 1928–1930
44. Ramachander, R., Kim, C. A., Phillips, M. L., Mackereth, C. D., Thanos, C. D., McIntosh, L. P., and Bowie, J. U. (2002) *J. Biol. Chem.* **277,** 39585–39593
45. Thanos, C. D., Goodwill, K. E., and Bowie, J. U. (1999) *Science* **283,** 833–836
46. Kyba, M., and Brock, H. W. (1998) *Dev. Genet.* **22,** 74–84
47. Santos N. C., Prieto, M., and Castanho, M. A. (1998) *Biochemistry* **37,** 8674–8682
48. White, S. H., and Wimbley, W. C. (1999) *Annu. Rev. Biophys. Biomol. Struct.* **28,** *319–365.*
49. Killian, J. A., and Heijne, G. V. (2000) *Trends Biochem. Sci.* **25,** 429–434
50. White, S. H., Ladokhin, A. S., Jayasinghe, S., and Hristova, K. (2001) *J. Biol. Chem.* **276,** 32395–32398
51. Gelb, M. H., Cho, W., and Wilton, D. C. (1999) *Curr. Opin. Struct. Biol.* **9,** 428–432
52. Kyte, J., and Doolittle, R. F. (1982) *J. Mol. Biol.* **157,** 105–132
53. Cserzo, M., Wallin, E., Simon, I., von Heijne, G., and Elofsson, A. (1997) *Protein Eng.* **10,** 673–676
54. Tabuchi, K., Biederer, T., Butz, S., and Sudhof, T. C. (2002) *J. Neurosci.* **22,** 4264–4273
55. Cho, W. (2001) *J. Biol. Chem.* **276,** 32407–32410
56. Kim, C. A., Gingery, M., Pilpa, R. M., and Bowie, J. U. (2001) *Nat. Struct. Biol.* **9,** 453–457
57. Kim, C. A., Phillips, M., Kim, W., Gingery, M., Tran, H. H., Robinson, M. A., Faham, S., and Bowie, J. U. (2001) *EMBO J.* **20,** 173–182
58. Green, J. B., Gardner, C. D., Wharton, R. P., and Aggarwal, A. K. (2003) *Mol. Cell* **11,** 1537–1548
59. Aviv, T., Lin, Z., Lau, S., Rendl, L. M., Sicheri, F., and Smibert, C. A. (2003) *Nat. Struct. Biol.* **10,** 614–621
60. Tanaka Hall, T. M. (2003) *Nat. Struct. Biol.* **10,** 677–679
61. DeLano, W. L. (2002) *The PyMOL Molecular Graphics System*, DeLano Scientific, San Carlos, CA